Supporting Information

Harper et al. 10.1073/pnas.1105852108

SI Materials and Methods

Immunohistochemistry, Multispectral Imaging Analysis, and X-Gal Staining. Sections were dewaxed in Histoclear, rehydrated, and blocked in 1.5% hydrogen peroxide, boiled for 1 h in Tris-EDTA buffer (10 mM Tris base, 1 mM EDTA solution), blocked in 2% BSA/PBS solution before overnight incubation in primary antibody, washed, incubated in secondary antibody for 30 min (Envision kit; DAKO), developed via DAB, counterstained with hematoxylin (Vector Labs), dehydrated, and mounted in Cytoseal (Thermo Scientific). The following antibodies were used: Blimp1 (1:200; sc-130917; Santa Cruz), Ki67 (1:200; NCL-L-Ki67-MM1; NovoCastra), c-Myc (1:200; sc-764; Santa Cruz), Mucin-2 (1:100; sc-15334; Santa Cruz), and chromogranin (1:400; ab15160; Abcam). Alkaline phosphatase staining was carried out by using a kit from Vector Laboratories (SK-5100) per manufacturer instructions. For multispectral imaging analysis, sections were incubated in secondary antibodies conjugated directly to quantum dots (Molecular Probes/Invitrogen) for 1 h, washed, dehydrated, and mounted. Images were taken by using a Nuance MSI camera (LOT; Oriel). X-gal staining was carried out as described (1).

Western Blot Analysis. E18.5 intestinal tissue was homogenized in radioimmunoprecipitation assay lysis buffer containing a mixture of protease inhibitors (Sigma). Proteins (50 μg) were resolved on 8% SDS/PAGE gels, transferred to PVDF membranes (Millipore), blocked for 1 h in TBS with Tween-20 containing 7% nonfat dry milk, and sequentially probed with monoclonal rat anti-Blimp1 antibody (sc-130917; Santa Cruz), followed by ECL goat anti-rat IgG (Amersham). Blots were then stripped and reprobed with rabbit anti–β-tubulin (sc-9104; Santa Cruz) to confirm equal protein loading.

1. Nagy A, Gertsenstein M, Vintersten K, Behringer R (2003) Manipulating The Mouse Embryo: A Laboratory Manual (Cold Spring Harbor Lab Press, Cold Spring Harbor, NY).

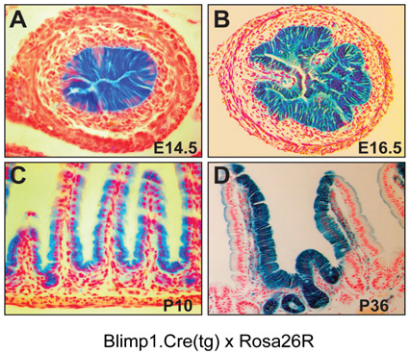

Fig. S1. Blimp1^{-} adult crypt stem cells derive from Blimp1^{+} fetal progenitors. (*A*) X-gal staining throughout *Blimp1.Cre*(*tg*) x *Rosa26R* primitive gut endoderm at E14.5. (*B* and *C*) The fetal epithelium remains positive in utero. (*D*) In adults, the entire crypt villous axis contains labeled progeny.

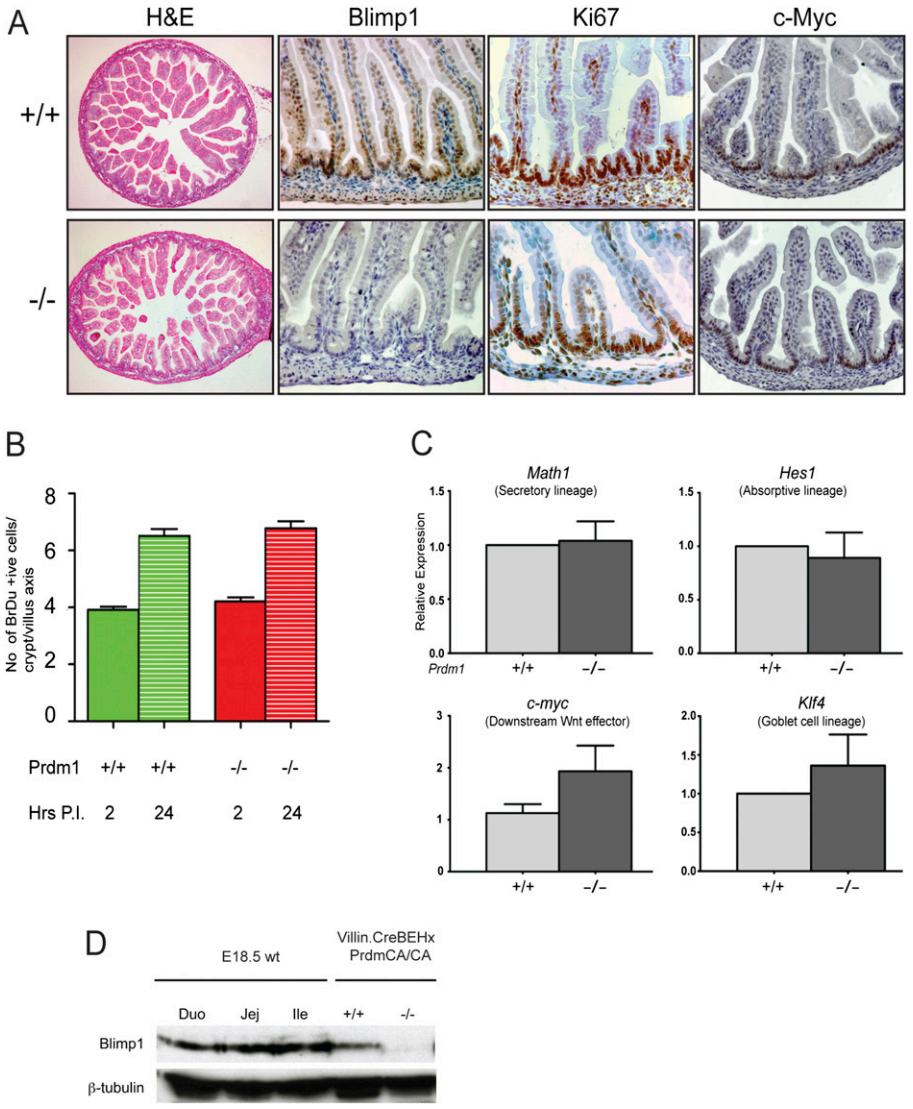

Fig. S2. Conditional inactivation eliminates Blimp1 expression but has no noticeable effect on terminally differentiated cell types or cell proliferation at E18.5. (*A*) H&E, Blimp1, Ki67, and c-Myc staining of WT and mutant proximal SI sections. (*B*) BrDU^{+} cell counts at 2 or 24 h postinjection (P.I.) confirms equivalent rates of proliferation. (*C*) qPCR analysis of intestinal regulators revealed no significant differences between control and mutants ($n > 8$ for both genotypes). (*D*) Western blot analysis of E18.5 WT intestine shows roughly equivalent Blimp1 expression levels in all segments, whereas conditional mutants lack expression. Blots were stripped and reprobed for β-tubulin to ensure equal protein loading.

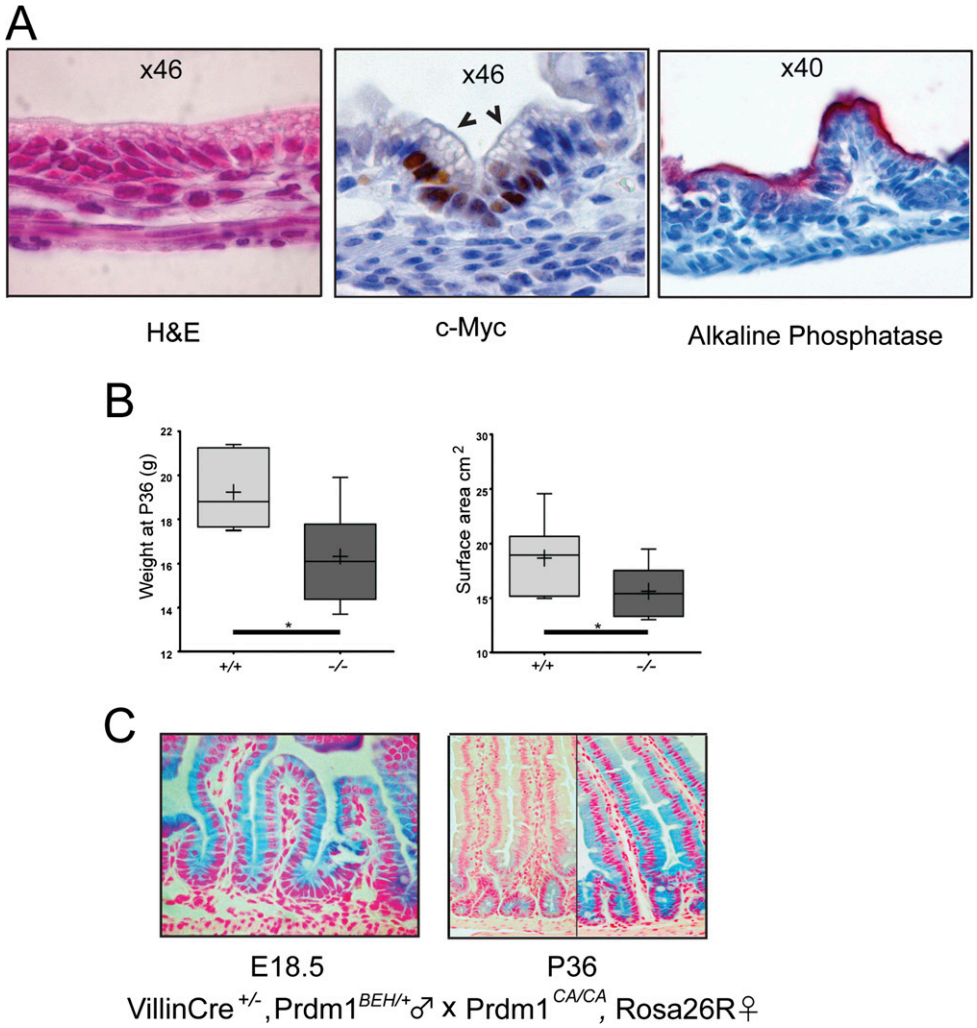

Fig. S3. Blimp1 loss causes fetal intestinal epithelial cells to acquire a terminal columnar phenotype, reduced villus density, and growth retardation. (*A*) H&E staining of mutant SI at P3 reveals the intervillous regions occupied by differentiated columnar epithelium. c-Myc^{+} cells confined to the rare shallow crypts are columnar and highly vacuolated (arrows) and uniformly express alkaline phosphatase. (*B*) Survivors display decreased body weights and reduced SI surface area (box, interquartile range; horizontal line, median; vertical line, minimum to maximum values excluding outliers; cross, mean; $n > 9$ for both genotypes). (*C*) Monitoring Villin.Cre-mediated deletion activity via X-gal staining shows the majority of the epithelium of the intestine and colon is deleted at E18.5. Survivors show areas of LacZ staining and nonstaining tissue suggesting transgene silencing or repopulation of neonatal epithelium by WT cells. As Blimp1 is not expressed in mature crypts, Villin.Cre-mediated deletion in adults has no physiological consequence.

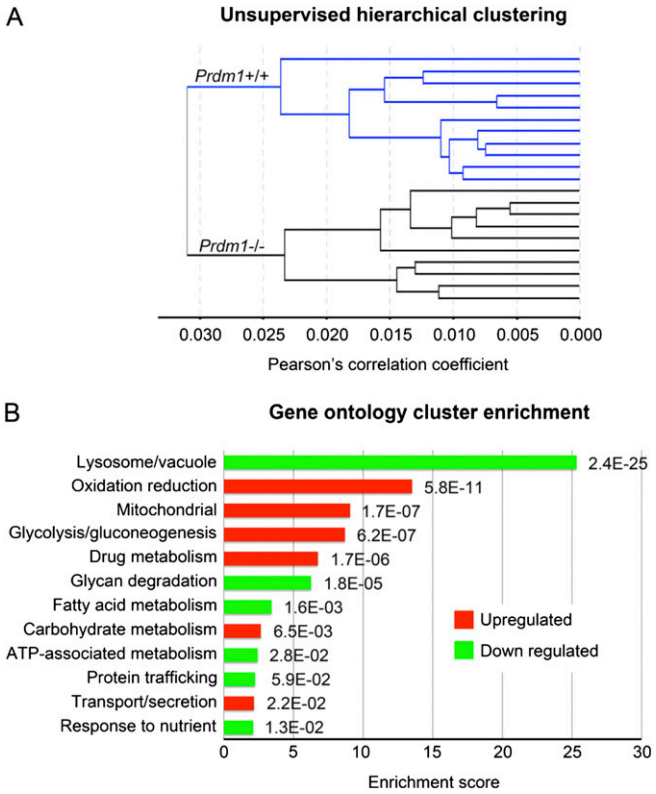

Fig. S4. Array data analysis. (*A*) Unsupervised hierarchical clustering of *Prdm1*$^{+/+}$ and *Prdm1*$^{-/-}$ SI array samples. Clear separation of Prdm1 genotypes illustrates a high level of divergence between WT and mutant samples. (*B*) Functional annotation clustering analysis (DAVID 6.7) of up- and down-regulated genes from *Prdm1*$^{-/-}$ SI identifies enrichment of multiple gene clusters associated with energy metabolism, vacuole function, and molecular transport. The statistical significance of enrichment for each cluster is indicated by the *P* value indicated at the end of each bar on the graph.

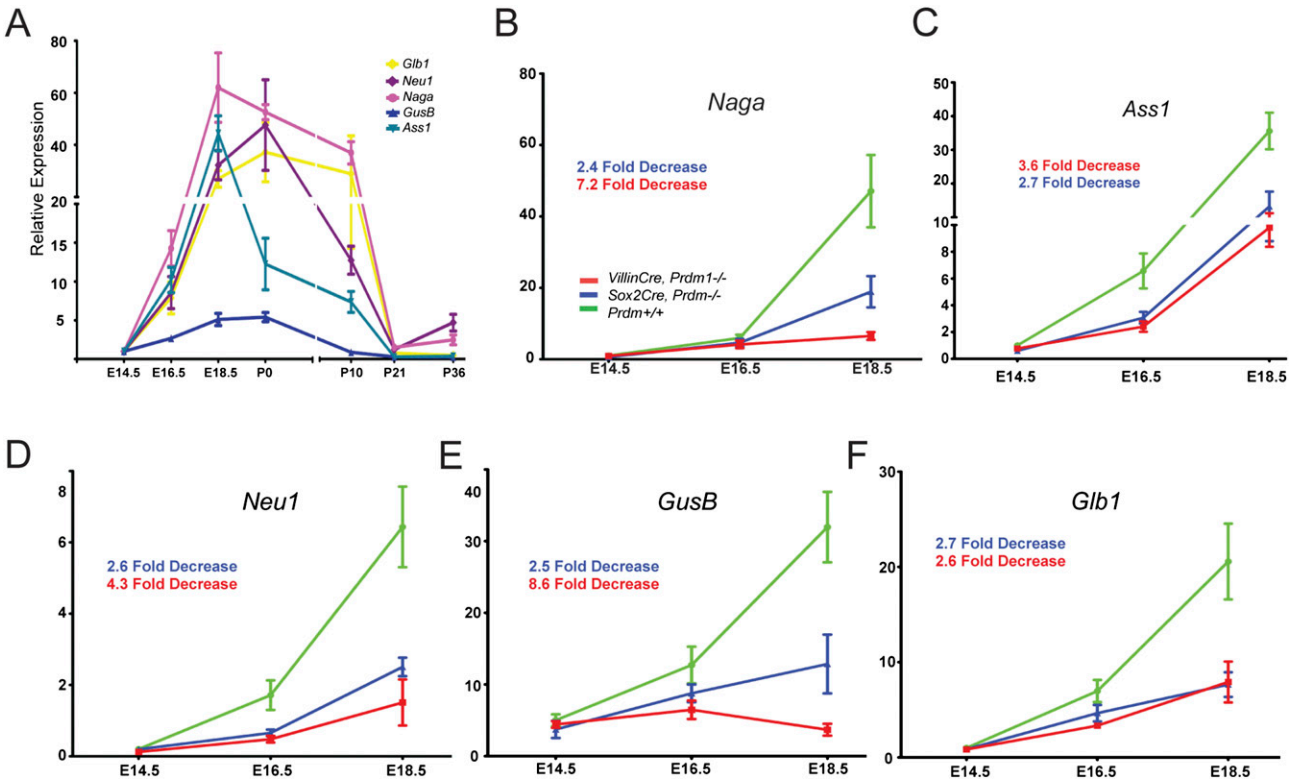

Fig. S5. Blimp1 loss compromises expression of immature enterocyte markers. (*A*) qPCR analysis of juvenile enterocyte markers. WT transcriptional profiles dramatically change between P10 and P21 as adult enterocytes repopulate the villus axis. (*B–F*) Expression of the immature markers *Naga*, *Ass1*, *Neu1*, *GusB*, and *Glb1*, is markedly reduced in mutant samples (green line, control; red line, *VillinCre* mutant; blue line, *Sox2Cre* mutant; symbol, mean; vertical line, ± SEM; $n \geq 10$ for all genotypes).

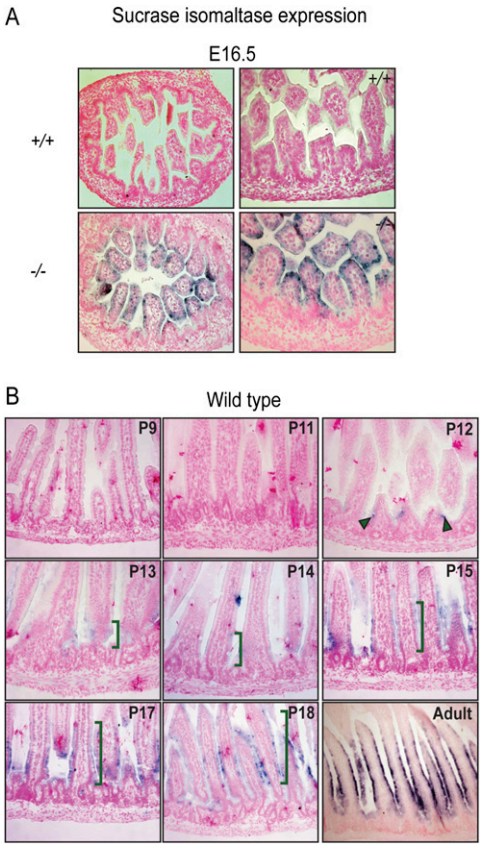

Fig. S6. The onset of *Sis* expression normally coincides with crypt maturation and the emergence of Blimp1^{-} adult enterocytes. (*A*) In situ hybridization at E16.5 shows WT enterocytes lack expression, whereas *Sis* is activated prematurely in Blimp1 mutant SI. (*B*) In WT postnatal intestines, expression is undetectable until P12, when a few *Sis*$^{+}$ cells exiting the crypt villus junction become visible (green arrows). The *Sis*$^{+}$ domain rapidly expands as Blimp1^{-} adult enterocytes migrate up the villi. By P18, and continuing into adulthood, *Sis*$^{+}$ enterocytes represent the predominant population.

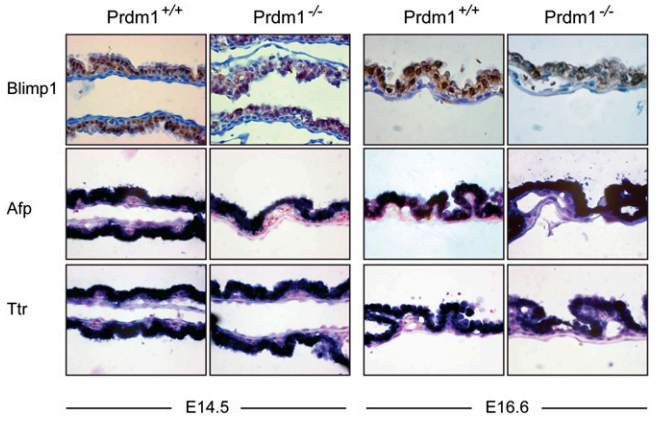

Fig. S7. Blimp1-independent Afp and Ttr expression in the yolk sac endoderm. (*A*, *B*, *G*, and *H*) At E14.5 and E16.5, Blimp1 is strongly expressed in WT visceral yolk sac endoderm but not in *Villin.Cre*-deleted embryos. (*C*–*F* and *I*–*L*) *Afp* and *Ttr* expression is unaffected in mutant yolk sac endoderm.

Table S1. Recovery of correct Mendelian ratios of all possible genotypes at E18.5 and P0

Parameter	$Prdm1^{CA/+}$	Villin $Cre^{+/-}$, $Prdm1^{CA/+}$	$Prdm1^{CA/BEH}$	Villin Cre, $Prdm1^{CA/BEH}$
Prdm1 dosage	+/+	+/–	+/–	–/–
E18.5 (n = 112)				
Expected (E)	28	28	28	28
Observed (O)	30	29	28	25
O – E	2	1	0	-3
$(O - E)^2$	4	1	0	9
$(O - E)^2 / E$	0.142857143	0.035714286	0	0.321428571
P0 (n = 179)				
Expected (E)	44.75	44.75	44.75	44.75
Observed (O)	45	49	44	41
O – E	0.25	4.25	–0.75	–3.75
$(O - E)^2$	0.0625	18.0625	0.5625	14.0625
$(O - E)^2 / E$	0.001396648	0.403631285	0.0125698	0.31424581

For E18.5, $\chi^2 = 0.5$, P = NS. For P0, $\chi^2 = 0.731844$, P = NS. The expected genotypes were recovered at correct Mendelian ratios from Villin-Cre, Prdm1BEH/+, Prdm1CA/CA matings at E18.5 and P0. χ^2 test with 3 degrees of freedom.

Table S2. Partial list of misregulated transcripts identified in E18.5 Blimp1 mutant intestines

Function gene	Chr	Gene name	Fold change (array)	Mean fold change (qPCR)	Predicted Blimp-1 BS
Up-regulated					
Metabolism					
Arg2	12	Arginase-2	282.08	39	1
2010204N08Rik	3	Sucrase Isomaltase	128.83	118	5
Cyp4v3	8	Cytochrome P450, family 4, subfamily v, polypeptide 3	27.67	25.57	0
Reg3a	6	Regenerating Islet derived-3A	13.29		
Gsta1	9	GST-1	11.71	2.86	1
Gsta4	9	GST-4	7.47	6.79	3
Gsta2	9	GST-2	5.44	2.49	0
Reg1	6	Regenerating Islet derived-1	5.09	7.7	3
Cyp2d26	15	Cytochrome P450, family 2, subfamily d, polypeptide 26	5.06		1
Reg3b	6	Regenerating Islet derived-3B	4.96		1
Treh	9	Trehalase	4.79	3.4	0
Aldh1a1	19	Aldehyde dehydrogenase 1 family, member A1	4.67		3
Dpep1	8	Dipeptidase-1	3.63		2
Molecule transport					
Aqp3	4	Aquaporin-3	16.29	4.66	0
Slc16a5	11	Solute carrier family 16 (monocarboxylic acid transporters), member 5	16.07		2
Slc5a8	10	solute carrier family 5 (iodide transporter), member 8	5.14		
Slc46a1	11	Solute carrier family 46 (folate transporter), member 1	3.59		0
Cell adhesion/ECM					
Myo18b	5	Myosin 18B	16.5		
Krt20	11	Keratin 20	2.7		0
Gal3st2	1	Galactose-3-*O*-sulfotransferase 2	2.49		3
Myo1a	10	Myosin IA	2.24	4	0
Unknown					
1810065E05RIK	11	RIKEN cDNA 1810065E05 gene	118.16	24.35	5
2210407C18RIK	11	RIKEN cDNA 2210407C18 gene	15.69	67.21	6
Down-regulated					
Metabolism					
Afp	5	α-Fetoprotein	29.3	27.7	2
Ttr	18	Transthyretin	6.27	2.99	1
Pgam2	11	Phosphoglycerate mutase 2	5.96		1
Trf	9	Transferrin	4.71		1
Gusb	5	Glucuronidase, β	3.82	8.5	1
Naga	15	*N*-acetyl galactosaminidase, α	2.88	7.2	4
Asl	5	Arginosuccinate lyase	2.51		1
Ass1	2	Argininosuccinate synthetase 1	2.42	3.6	4
Neu1	17	Neuraminidase 1	1.85	4.3	0
Glb1	9	Galactosidase, β	1.7	2.6	1
Cell adhesion/ECM					
Fndc5	4	Fibronectin type III domain containing 5	9.06		2
Lrrn1	6	Leucine rich repeat protein 1, neuronal	5.18		1
Krt23	11	Keratin 23	4.77		3

Fold change differences ($P < 0.05$) observed in Illumina microarray analysis were validated by qPCR analysis where indicated. Blimp1 binding site (BS) predictions are based on algorithms from Genomatix software. Chr, chromosome.

Table S3. Primer and probe set used for qPCR

Gene name	Primer pair sequence	Universal probe library probe no.
Hes1	TGCCAGCTGATATAATGGAGAA	83
	CCATGATAGGCTTTGATGACTTT	
c-myc	CCTAGTGCTGCATGAGGAGA	77
	TCCACAGACACCACATCAATTT	
Klf4	GGACTCCGGAGGACCTTCT	83
	GAGAAGGACGGGAGCAGAG	
Actin	AAGGCCAACCGTGAAAAGAT	56
	GTGGTACGACCAGAGGCATAC	
Prdm1 (*Exon4-5*)	AGTTCCCAAGAATGCCAACA	31
	TTTCTCCTCATTAAAGCCATCAA	
Math1	TGCGATCTCCGAGTGAGAG	69
	CTCTTCTGCAAGGTCTGATTTTT	
Sis	GGTGAGCAGTGCAACAAAGA	16
	CAGGACATTCAACACCATTGA	
Gsta1	CCGGAAGATTTGGAAAAGC	21
	TTTGGTGGCGATGTAGTTGA	
Cyp4v3	TGGCTGGGACTAGGACTTCTT	69
	TGGAAAGTGGGCGTTAGC	
Gsta4	CCAGCTCCTAGAAGCCATTTT	31
	GGAATGTTGCTGATTCTTGTCTT	
Gsta2	CAGAGTCCGGAAGATTTGGA	22
	AGAATGGCTCTGGTCTGCAC	
Reg1	TGGCTAGGAACGCCTACTTC	108
	CTTCTGGGCAACTGATCCTG	
Aqp3	GGCTGGGGCTCAGAAGTC	77
	GAAGACACCAGCGATGGAAC	
1810065E05RIK	AATCAAGTGGACACGAAACCA	16
	TGCACTTCAGAGGAGTTGGA	
Ttr	GACTGGTATTTGTGTCTGAAGCTG	56
	TTACAGCCACGTCTACAGCAG	
Afp	AGTGCGTGACGGAGAAGAA	69
	AGCCAACACATCGCTAGTCA	
Myo1A	CGTGATCAACTACTGCAATGAGA	62
	TCCACCTTTGTCCACGGTAT	
Treh	GCTGGGGCTGGGACTTAG	77
	TCTCCATGGCAGTAGATCTGG	
Glb1	TGCTCTTCGAGAAGTCATTCAG	95
	TGGGTGTAGACGGAGGGATA	
Neu1	GACCTGGCTCAGGCATTC	94
	GGCACCGTGGTCATCACT	
Naga	TGCCTTCCTAGCTGACTATGC	105
	GTCATTTTGCCCATGTCCTC	
GusB	CAGGGTCAACTTCAGGTTCC	49
	CAGTTGTTGTCACCTTCACCTC	
Arg2	TATGGTCCAGCTGCCATTC	80
	CCAAAGTCTTTTAGGTGGCATC	
Ass1	TGGCCAGGAAAGCAGACTAC	49
	ACGAGGATGCAGGAGGTGT	